Theoretical Investigations of Anion−π Interactions: The Role of Anions and the Nature of π Systems

Dongwook Kim, P. Tarakeshwar,* and Kwang S. Kim*

National Creative Research Initiative Center for Superfunctional Materials, Department of Chemistry, Division of Molecular and Life Sciences, Pohang University of Science and Technology, San 31, Hyojadong, Pohang 790-784, Korea

Received: November 27, 2003

The nature of the anion−π interaction has been investigated by carrying out high level ab initio calculations of the complexes of halide (F^-, Cl^-, and Br^-), linear organic (CN^-, NC^-), and trigonal planar organic (NO_3^- and CO_3^{2-}) anions with different kinds of π systems, viz. olefinic (tetrafluoroethene), aromatic (hexafluorobenzene), and heteroaromatic (1,3,5-triazine). In an effort to comprehend the underlying basis of this interaction, we have also carried out a rigorous decomposition of the interaction energies using the symmetry adapted perturbational theory (SAPT) method. Contrary to our expectations, the results indicate that the magnitudes of total interation energies of anion−π and cation−π interactions are similar. In contrast to cation−π interactions, anion−π interactions are, however, marked by substantial contributions from dispersion energies. As in the case of cation−π interactions, the role of anions also have a marked influence on the nature and magnitude of the anion−π interaction with interactions involving halide anions being dominated by electrostatic and the induction energies. On the other hand, dispersion energies are markedly higher in interactions involving organic anions. Apart from aiding an understanding of the origin of anion−π interaction, we believe that the present results would help understand the basis of biomolecular structures and enzyme−substrate interactions and also aid the design of new drugs and novel ionophores/receptors.

1. Introduction

There has been a lot of interest in the design and development of precise functional devices in the nano and sub-nano scale,[1−5] in the recent past. The fact that the structures and properties of these nanosystems and several biological systems are to a large extent governed by the nature of the intermolecular interactions prevailing in them[6−11] has spurred a number of investigations detailing the nature of several intermolecular interactions.

In this context, it is interesting to note that most of the investigations to date are devoted to systems involving either cations or neutral molecules. Interactions involving anions have received considerably lower attention, because it is relatively easier to investiate electron-deficient units both experimentally and theoretically.[12] Nevertheless, during the last two decades, a number of experimental investigations have detailed the efforts to design receptor molecules involving anions, because of the potential role of such receptor molecules in vast areas of biology, medicine, catalysis, and enviromental science. However, the repertoire of systems harnessed to bind anions is still limited. In particular, systems containing aromatic π systems have received scant attention because they are generally considered to be electron-rich and hence were expected to exhibit repulsive interaction with anions.

However, several recent reports describing the interactions of the π-cloud of hexafluorobenzene with electron-donating sites of heteroatomic moleculues such as H_2O, HCN, HF, etc.,[13−15] seem to indicate that that these electron deficient π systems could serve as interesting receptor molecules capable of binding anions. In this connection, there has been a recent theoretical report of the interaction of these electron-deficient π systems with several anions.[16−20] In particular, Quinonero et al. provide evidence of the existence of these interactions in crystal structures, through a systematic search of the Cambridge Structural Database (CSD).[17,18] Recently, Mascal et al.[19] proposed a heteroatomic aromatic molecule, 1,3,5-triazine, as a π-deficient molecule capable of binding anions, and Alkorta et al.[20] reported the interaction of some anions with several perfluoro aromatic compounds.

To the best of our knowledge, all the above studies have focused their attention on the feasibility of aromatic π systems binding anions. To date, there have been no investigations on the interactions of olefinic π systems and anions. Furthermore, there has been no systematic and comprehensive investigations of the role of both the anions and the π system on the nature of the ensuing anion−π interaction.

Toward this end, the present study details a comprehensive investigation of the interaction of various anions with several representative π systems. We selected three molecules (tetrafluoroethene, hexaflurobenzene, and 1,3,5-triazine) as models for three different categories of π systems (olefinic, aromatic, heteroaromatic). In addition to their complexes with spherical monatomic halide ions (F^-, Cl^-, and Br^-), we also investigated complexes with linear anion (both ends of CN^-) and trigonal planar anions (NO_3^- and CO_3^{2-}). Apart from an evaluation of the equilibrium geometries, interaction energies, and vibrational frequencies, we also focus our attention on a quantitative estimation of the individual interaction energy components. The utilitiy of these quantitative estimates in obtaining a detailed insight into the nature of interactions involving π systems has been highlighted in recent work from our group.[21−24]

* Corresponding authors. E-mail: (P.T.) tara@postech.ac.kr, (K.S.K.) kim@postech.ac.kr.

10.1021/jp037631a CCC: $27.50
Published on Web 01/22/2004

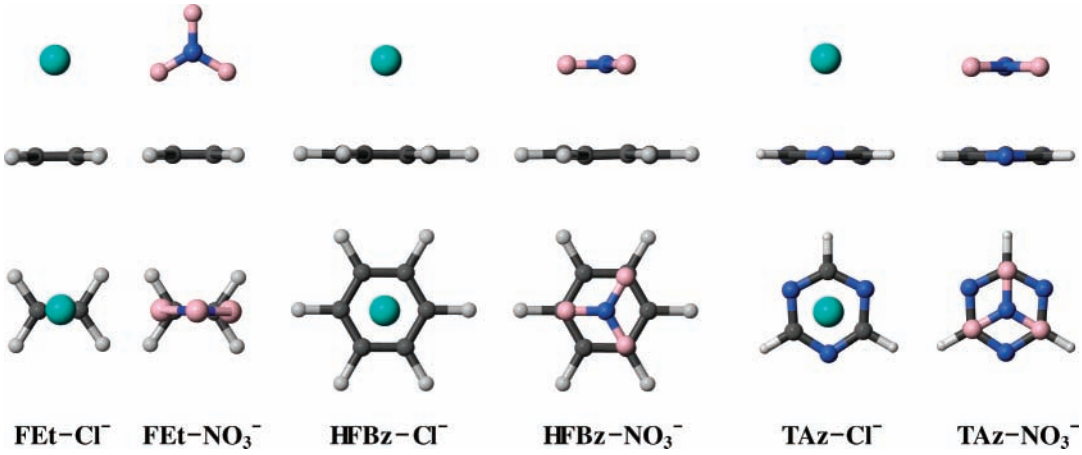

Figure 1. MP2/aug-cc-pVDZ optimized structures of Cl^- and NO_3^- complexes with π systems investigated in this study. The structures in the top layer are depicted from the side view, and those in the bottom layer from the top view.

2. Methods

All the results presented in this work were produced by employing either supermolecular (SM) variational or symmetry adapted perturbation theory (SAPT) methods.[25,26] Although the SM method is conceptually and computationally simple, it does not provide a clear picture of interaction forces. On the other hand, the SAPT method computes the interaction energy directly as a sum of electrostatic, exchange repulsion, induction, and dispersion contributions so that a physical interpretaion of the interactions between the complex monomers can be evinced. We briefly elaborate the calculational details to aid the discussion of results.

2.1. Supermolecular Calculations. All the SM calculations were carried out at the second-order Møller−Plesset (MP2) level of theory using the 6-31++G** and aug-cc-pVDZ basis sets. Consequent to the suggestions of a referee, we have also carried out single point calculations, on some of the smaller complexes, at the coupled-cluster with single, double, and perturbative triple substitutions [CCSD(T)] levels of theory to examine the effects of the inclusion of higher levels of correlation. All the electrons were explicitly correlated in the MP2 and CCSD(T) calculations. The geometries of all the complexes were optimized with proper symmetry constraints so that the center of anion lies along the principal axes of π systems (C_2 axis for tetrafluoroethene, C_6 axis for hexafluorobenzene, and C_3 axis for 1,3,5-triazine). The representative structures obtained by optimization of the complexes of Cl^- and NO_3^- with the three π molecules considered in this study are shown in Figure 1. Basis set superposition error (BSSE) corrections for all these complexes were carried out using the counterpoise (CP) method of Boys and Bernardi.[27] The zero point vibrational energy (ZPVE) corrections were calculated using the frequencies evaluated at the MP2/6-31++G** and MP2/aug-cc-pVDZ levels of theory.

Recent reports[28,29] seem to indicate that the charges evaluated using the atomic polar tensors (APT) are more representative of the electron density distributions and are also relatively insensitive to basis set variations.[29] Hence, to carry out charge analysis, we have computed the APT charges from the calculated wave functions of the optimized geometries of these complexes.

The SM calculations were carried out using the GAUSSIAN suite of programs.[30]

2.2. Symmetry Adapted Perturbation Theory Calculations. In this study, the SAPT calculations were carried out using the optimized geometries of all the complexes obtained from SM calculations at MP2/aug-cc-pVDZ level. The SAPT interaction energy accurate to the third order, E_{int}, is given by

$$E_{int} = E_{es}^{(1)} + E_{exch}^{(1)} + E_{ind}^{(2)} + E_{exch-ind}^{(2)} + E_{disp}^{(2)} + E_{exch-disp}^{(2)} + \delta_{int}^{HF} \quad (1)$$

$$= E_{es} + E_{exch} + E_{ind} + E_{disp} \quad (2)$$

where

$$E_{exch} = E_{exch}^{(1)} + E_{exch-ind}^{(2)} + E_{exch-disp}^{(2)} + \delta_{int}^{HF}$$

and where $E_{es}^{(1)}$ is the electrostatic energy of monomers with the unperturbed electron distributions, $E_{exch}^{(1)}$ is their first-order valence repulsion energy due to the Pauli exclusion principle, $E_{ind}^{(2)}$ stands for the second-order energy gain resulting from the induction interaction, $E_{exch-ind}^{(2)}$ represents the repulsion change due to the electronic cloud deformation, $E_{disp}^{(2)}$ is the second-order dispersion energy, $E_{exch-disp}^{(2)}$ denotes the second-order correction for a coupling between the exchange repulsion and the dispersion interaction, and δ_{int}^{HF} includes the higher order induction and exchange corrections. For the sake of brevity, the exchange term E_{exch}, represents the sum of the four terms, $E_{exch}^{(1)}$, $E_{exch-ind}^{(2)}$, $E_{exch-disp}^{(2)}$, and δ_{int}^{HF}. Because BSSE effects are explicitly included when the SAPT interaction energies are evaluated, a comparison of BSSE corrected supermolecular interaction energy (ΔE_e^B) and the SAPT interaction energy (E_{int}) is appropriate.

Given the size of the systems and the level of theory employed in this study, it was not feasible to evaluate the computationally demanding higher order components using the same basis sets as those of SM calculations. Hence, we not only reduced the size of basis sets by using hybrid basis sets but also restricted the order of energy components ($n \leq 3$). The hybrid basis sets are composed of the 6-31G** basis sets for F atoms of perfluoro−π molecules and the 6-31+G* basis sets for the rest of atoms, which is identical to 6-31++G** except for H and He atoms. Accordingly, one should expect a slight deviation of the total interaction energies evaluated using SAPT and SM calculations. This, however, does not affect our conclusions based on the magnitude of the individual interaction energy components, as was shown in recent papers.[21,23] A detailed description of SAPT and some of its applications can be found in some recent references.[25,31−33]

3. Results and Discussion

The geometries of all the representative complexes, which were optimized with proper symmetry constraints, i.e., C_{2v} for

TABLE 1: Total Binding Energies and Selected Geometries Obtained at the MP2 Level Using 6-31++G and aug-cc-pVDZ for Various Anion−π Complexes[a]**

	F^-	Cl^-	Br^-	CN^-	NC^-	NO_3^-	CO_3^{2-}
				$\pi = C_2F_4$			
$R_\perp$	2.58 (2.54)	3.18 (3.13)	3.36 (3.29)	3.14 (3.07)	2.94 (2.88)	3.38 (3.31)	3.04 (3.01)
$-\Delta E_e$	10.73 (11.14)	5.84 (7.00)	5.49 (6.03)	5.97 (6.31)	6.31 (6.68)	7.09 (7.78)	18.84 (20.66)
$-\Delta E_0$	10.52 (10.94)	5.69 (6.84)	5.35 (5.90)	5.72 (6.02)	6.10 (6.46)	6.49 (7.11)	18.59 (20.35)
$-\Delta H_{298}$	11.08 (11.49)	6.16 (7.33)	5.23 (5.77)	5.66 (6.00)	7.18 (7.54)	5.86 (7.13)	18.57 (20.37)
$-\Delta E_{corr}$	1.88 (2.32)	4.15 (4.11)	3.92 (5.07)	2.52 (3.77)	1.99 (3.13)	4.47 (5.90)	9.88 (11.89)
				$\pi = C_6F_6$			
$R_\perp$	2.57 (2.52)	3.15 (3.05)	3.29 (3.19)	2.98 (2.91)	2.80 (2.80)	2.91 (2.59)	2.71 (2.67)
$-\Delta E_e$	18.87 (18.40)	12.97 (13.98)	12.68 (12.72)	13.06 (12.97)	13.38 (13.30)	12.73 (13.94)	32.83 (34.79)
$-\Delta E_0$	17.54 (18.05)	11.48 (13.58)	11.26 (12.14)	11.44 (12.03)	11.84 (12.39)	10.93 (12.32[b])	31.23 (33.21[b])
$-\Delta H_{298}$	18.59 (19.24)	11.42 (13.61)	11.15 (12.75)	10.91 (11.75)	12.45 (13.26)	10.23 (11.93[b])	31.69 (33.99[b])
$-\Delta E_{corr}$	3.42 (3.50)	8.60 (7.44)	8.44 (9.26)	6.77 (7.67)	5.60 (6.53)	12.68 (14.52)	16.40 (18.22)
				$\pi = C_3N_3H_3$			
$R_\perp$	2.59 (2.54)	3.22 (3.13)	3.39 (3.29)	3.06 (2.97)	2.85 (2.78)	3.00 (2.90)	2.76 (2.70)
$-\Delta E_e$	9.75 (10.59)	5.23 (6.93)	5.20 (5.99)	5.84 (6.63)	6.47 (7.29)	5.34 (6.79)	16.84 (20.07)
$-\Delta E_0$	9.52 (10.56)	5.00 (6.83)	5.07 (5.93)	5.35 (6.19)	5.96 (6.95)	4.66 (6.26)	16.46 (19.82)
$-\Delta H_{298}$	9.42 (11.61)	4.95 (6.75)	4.98 (5.83)	6.04 (5.78)	6.66 (7.64)	4.03 (5.65)	17.03 (20.43)
$-\Delta E_{corr}$	3.83 (4.96)	6.52 (7.40)	6.35 (8.63)	4.84 (7.02)	4.97 (7.06)	9.31 (12.24)	13.31 (17.47)

[a] All energies are in kcal/mol and all distances are in ångstroms. $R_\perp$ represents the perpendicular distance from the center-of-mass of the π ring to the anion (the anion position of CN^- or NC^- corresponds to the atom in contact with the π system, and those of NO_3^- and CO_3^{2-} to the central atom of anion, i.e., N and C, respectively). CN^- and NC^- denote that C and N contact with π systems, respectively. The values evaluated at the MP2/aug-cc-pVDZ level are in parentheses. "$-\Delta E_e$" represents the binding energies with BSSE correction. "ΔE_0" is the ZPVE-corrected ΔE_e. "ΔH_{298}" is the enthalpy at 298.15 K and 1.0 atm. The electron correlation energy ΔE_{corr} is E_e(MP2) subtracted by E_e(HF) at the MP2 optimized geometry. [b] These values have been obtained using the ZPVE and thermal corrections evaluated at the MP2/6-31++G** level.

tetrafluoroethene (**FEt**) complexes, C_{6v} or C_{3v} for hexafluorobenzene (**HFBz**), and C_{3v} for 1,3,5-triazine (**TAz**), are shown in Figure 1. The vibrational frequencies were also calculated for the optimized geometries. The frequencies indicate that only a few complex structures where the anion directly interacts with the π cloud are genuine minima (for **FEt**, complex of Br^-; for **HFBz**, those of Cl^-, CN^-, and NO_3^-; for **TAz**, those of Cl^-, Br^-, and NO_3^-). For several complexes (for **FEt**, complex of NO_3^-; for **HFBz**, that of Br^-; for **TAz**, that of CN^-), the Hessians were extremely dependent on the kind of basis set employed. In the case of the remaining, the genuine minimal energy structures correspond to the nucleophilic attack of an anion with one of carbon atoms of π systems. However, because the ultimate aim of this study is to verify the anion recognizing propensity of these electron-depleted π systems, and to obtain an insight into the nature of the interaction, we only concentrate on those complex geometries, wherein the anions are located along the principal axes of the π system.

The value of interaction energies (ΔE_e and ΔE_0), interaction enthalpies (ΔH_{298}), and intermolecular distances ($R_\perp$) for the optimized geometries of all the anion−π complexes in this study, evaluated at the MP2/6-31++G** and MP2/aug-cc-pVDZ levels of theory, are listed in Table 1. The data indicate that for complexes of a halide anion, the interaction energies decrease as the sizes of anions increase, similar to those of complexes of alkali metal cations and π systems. The magnitude of interaction energies between halide ions and perfluoro−π systems (**FEt** and **HFBz**) is similar to that of the corresponding complexes of alkali metal cations and π systems (C_2H_4 and C_6H_6). For instance, the calculated interaction enthalpies ΔH_{298} of K^+−ethene and K^+−benzene complexes at MP2/6-31+G* in our previous study are −7.05 and −14.79 kcal/mol, respectively.[24] The corresponding values in this study of **FEt**−Cl^- and **HFBz**−Cl^- complexes are −6.16 and −11.42 kcal/mol.

However, the interaction between halide ions and π systems is expected to exhibit features different from those of the corresponding π-alkali metal cation complexes. In contrast to the cation−π interaction of alkali metal ions where the electrostatic and induction forces dominate the interaction,

TABLE 2: Total Binding Energies Obtained at CCSD(T)/aug-cc-pVDZ//MP2/aug-cc-pVDZ Levels for Several Tetrafluoroethene (FEt) Complexes of Anions[a]

	FEt−F^-	FEt−Cl^-	FEt−Br^-	FEt−CN^-	FEt−NC^-	FEt−NO_3^-
$-\Delta E_e$	11.82	6.85	5.79	6.20	6.67	7.74
$-\Delta E_0$	11.62	6.69	5.67	5.91	6.45	7.07
$-\Delta H_{298}$	12.17	7.18	5.54	5.89	7.53	7.09
$-\Delta E_{corr}$	3.19	3.91	4.67	3.63	3.11	5.94

[a] All energies are in kcal/mol. See the figure for the description of the complex forms. See footnote *a* of Table 1 for description of various terms. The ZPVE corrections have been evaluated using frequencies obtained at the MP2/aug-cc-pVDZ level of theory.

dispersion forces play an important role in the anion−π interaction. This is due to the high electron density and large ionic radii of halide anions compared to that of the alkali metal cations. A quick glance at the ratio of the correlation energy ΔE_{corr} to the BSSE corrected total interaction energy ΔE_e^B (even though ΔE_{corr} contains contributions from a number of energy terms, it gives an estimate of the dispersion energy) gives credence to the above assertion, with the calculated ratio of ΔE_{corr} to ΔE_e^B being 66% for the Cl^-−**HFBz** complex and 21% for K^+−benzene complex.[24]

Given the importance of dispersion energies, it is useful to examine the consequences of employing higher levels of correlation in evaluating the interaction energies. The CCSD(T) binding energies (Table 2) of the **FEt** complexes are very similar to the corresponding MP2 binding energies. More importantly, the relative trends in the interaction energies are very similar at both the MP2 and CCSD(T) levels. This finding reinforces our earlier observations that the MP2/aug-cc-pVDZ method is adequate in the description of the intermolecular interactions involving π systems.[23,26] Similar observations were also made by Tsuzuki et al., in their investigations of some π system containing complexes.[34]

There have been several attempts in the past to explain the origin of these anion−π interactions purely on electrostatic terms.[13,19,20] In the case of perfluoroarenes including hexafluorobenzene, the positive potential regions are observed above and below the molecular plane, whereas in the case of **TAz**,

TABLE 3: MP2 Equivalent Interaction Eneregy Components of All the Anion−π Complexes Obtained Using the Hybrid Basis Sets[a]

	F^-	Cl^-	Br^-	CN^-	NC^-	NO_3^-	CO_3^{2-}
				$\pi = C_2F_4$			
E_{int}	−8.72	−4.99	−4.31	−6.26	−6.35	−6.26	−19.15
E_{corr}	0.46	−1.68	−2.20	−3.11	−1.99	−2.85	−3.72
E_{es}	−20.93	−13.06	−12.22	−11.68	−10.43	−58.70	−15.30
E_{exch}	37.88	29.44	32.00	21.90	16.79	27.77	127.96
E_{ind}	−21.10	−17.64	−19.57	−12.77	−9.02	−12.49	−72.78
E_{disp}	−4.57	−3.74	−4.51	−3.71	−3.69	−6.24	−15.63
				$\pi = C_6F_6$			
E_{int}	−17.86	−12.92	−12.28	−15.47	−14.57	−11.67	−31.48
E_{corr}	0.77	−3.37	−4.68	−6.50	−3.81	−8.25	−7.90
E_{es}	−28.49	−22.71	−22.13	−22.73	−19.41	−19.67	−54.91
E_{exch}	42.54	43.44	48.72	38.38	27.93	35.08	106.10
E_{ind}	−25.39	−26.16	−29.54	−22.90	−15.57	−14.73	−61.48
E_{disp}	−6.52	−7.48	−9.33	−8.23	−7.52	−12.35	−21.19
				$\pi = C_3N_3H_3$			
E_{int}	−9.31	−5.39	−4.98	−7.15	−7.48	−4.84	−16.48
E_{corr}	−1.89	−4.25	−5.27	−5.98	−5.26	−7.00	−7.59
E_{es}	−18.74	−12.18	−11.50	−13.10	−11.38	−9.28	−33.77
E_{exch}	36.97	30.91	32.84	29.12	22.16	23.11	78.74
E_{ind}	−21.61	−18.13	−19.10	−16.63	−12.00	−9.15	−43.54
E_{disp}	−5.94	−5.99	−7.23	−6.54	−6.26	−9.53	−17.91

[a] All energies are in kcal/mol and evaluated at the MP2/aug-cc-pVDZ optimized geometries. The hybrid basis sets are composed of the 6-31G** basis sets for F atoms of C_2F_4 and C_6F_6, and the 6-31++G** basis sets for the other atoms. $E_{int} = E_{es} + E_{exch} + E_{ind} + E_{disp}$. E_{corr} is the sum of all the energy components evaluated at the correlated level.

they are located at near the C−H bond and centroid region. Quiñonero and co-workers tried to obtain a physical picture of the origin of anion−π interaction,[17,18] on the basis of an analysis of the electrostatic interaction of the negative charge of anion with the quadrupole moment of electron depleted π system, and the polarization effect of the π cloud. Though such an electrostatic representation provides a qualitative description, one does not obtain quantitative estimates. In particular, it is difficult to obtain the estimates of the dispersion energy, on the basis of such an electrostatic model.

Against this background, it is useful to compare the magnitude of various interaction energy components evaluated using the hybrid basis sets (Table 3). But before doing so, it is instructive to examine the reliability of these hybrid basis sets. In Figure 2, we plot the interaction energy components of the Br^- and NC^- complexes with **FEt**, obtained using the hybrid, 6-31++G**, and aug-cc-pVDZ basis sets. It can be seen that the increase in total interaction energy E_{int} obtained by using the larger basis set predominantly arises from an increase in the correlation energy contribution E_{corr}, which in turn is dominated by the dispersion energy E_{disp}. On the other hand, the changes in the induction energy E_{ind} and repulsive exchange energy E_{exch} are negligible. Similar conclusions can be drawn on the relative magnitudes of various interaction energy components, in the case of both the **HFBz** and **TAz** complexes. Interesting is the fact that substituting the 6-31G** basis set with 6-31++G** for the F atom of **FEt** gives rise to a larger increase in electrostatic energy (E_{es}) than substitution with aug-cc-pVDZ, which alters E_{es} little.

Armed with this information on the effect of basis sets, it is instructive to examine in detail the magnitude of the individual interaction energy component listed in Table 3 and plotted in Figure 3. In Figure 3, the interaction energy components of corresponding cation−benzene complexes (K^+−benzene complex for that of Cl^-−**HFBz**, and $C(NH_2)_3^+$−benzene complex for that of NO_3^-−**HFBz**) are also depicted to examine the

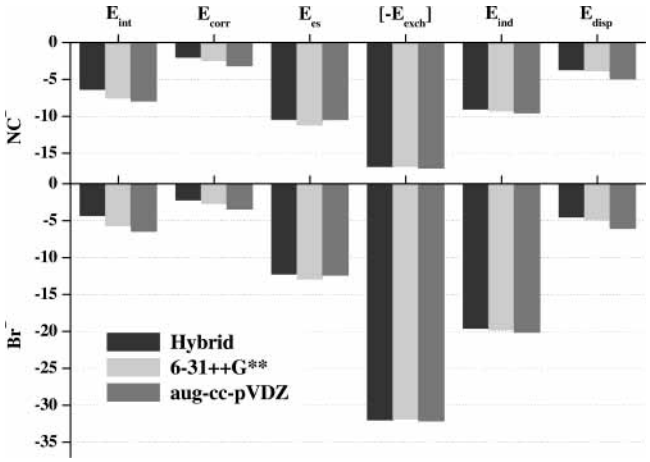

Figure 2. Comparison of the magnitude of the interaction energy components for Br^- and NC^- complexes with tetrafluoroethene evaluated using the hybrid, 6-31++G** and aug-cc-pVDZ basis sets. The hybrid basis set is composed of the 6-31G** basis sets for F atoms of C_2F_4 and the 6-31++G** basis sets for the other atoms. In the plot, E_{int} is the total interaction energy, E_{corr} is the interaction energy evaluated at the correlated level, E_{es} is the electrostatic energy, E_{ind} is the induction energy, E_{disp} is the dispersion energy, and E_{exch} is the sum of the all the exchange components ($E^{(1)}_{exch}$, $E^{(2)}_{exch-ind}$, $E^{(2)}_{exch-disp}$, and δ^{HF}_{int}).

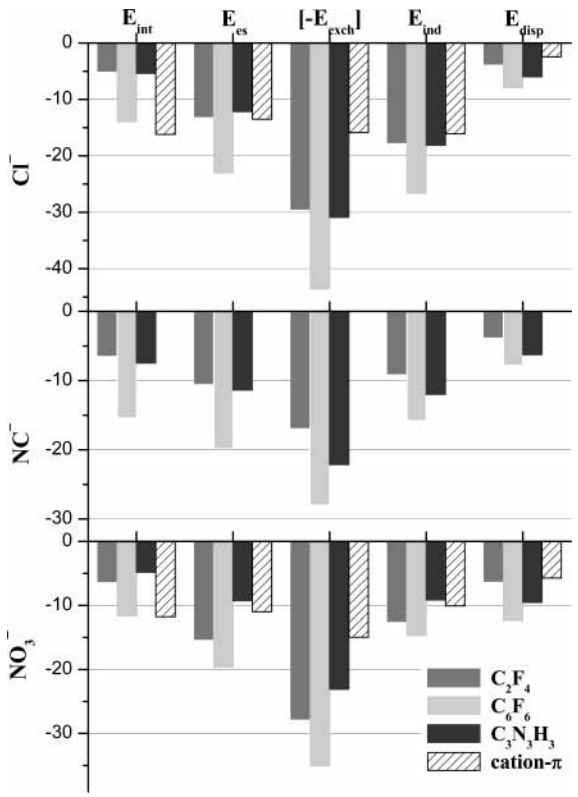

Figure 3. Comparison of the magnitude of the interaction energy components evaluated using the hybrid basis set for Cl^-, NC^-, and NO_3^- complexes with C_2F_4, C_6F_6, and $C_3N_3H_3$. As the cation−π complex corresponding to that of Cl^- with C_6F_6, data of the K^+−benzene complex are presented, and as the complex corresponding to that of NO_3^- with C_6F_6, data for $C(NH_2)_3^+$ are plotted.[27] The hybrid basis sets are composed of the 6-31G** basis set for F atoms of perfluoro−π systems, the 6-31++G** basis set for the other atoms. See the caption of Figure 2 and the text for the description of various interaction energy terms.

similarities/differences between anion−π interactions and the more well-known cation−π interactions.

Similar to the complexes of alkali metal cation with π systems, the major attractive contributions to total interaction

TABLE 4: APT Charge Transfer (Δq) from Anion to π Systems at the MP2/6-31++G* and MP2/aug-cc-pVDZ Levels[a]

	F^-	Cl^-	Br^-	CN^-	NC^-	NO_3^-	CO_3^{2-}
				6-31++G**			
C_2F_4	0.05	0.04	0.04	0.03	0.02	0.01	−0.03
C_6F_6	0.14	0.11	0.11	0.10	0.09	0.04	0.09
$C_3H_3N_3$	0.13	0.09	0.08	0.09	0.08	0.02	0.06
				aug-cc-pVDZ			
C_2F_4	0.04	0.04	0.05	0.04	0.02	0.01	−0.03
C_6F_6	0.14	0.11	0.11	0.11	0.10		
$C_3H_3N_3$	0.12	0.09	0.09	0.10	0.08	0.01	0.05

[a] Atomic polar tensor charges (au) are evaluated from the mean dipole moment derivatives.

energy emerge from the electrostatic E_{es} and induction E_{ind} energies for the complexes of halide anions. The electrostatic interaction predominantly arises from the interaction of the quadrupole moment of these π systems with the anions. The plots in Figure 3 indicate that in the case of benzene complexes, wherein the electrons are accumulated in the π cloud, the interaction is electrostatically repulsive. Therefore, the magnitude of electrostatic interaction gives a quantitative inkling of the depletion of π electron density. For instance, a comparison of the magnitude of electrostatic interaction between **HFBz** and **TAz** (the magnitude of the interactions of the former are nearly double that of the latter), indicates that the electron density in π cloud would be less depleted in the latter than in the former.

The induction energy can be described to result from the interaction between the highest occupied molecular orbital (HOMO) and the lowest unoccupied molecular orbital (LUMO). In these anion$-\pi$ complexes, the induction energy emerges from an interaction of the occupied p orbital for halide anions or π orbital for organic anions and the LUMO of the π systems. This inductive type of interaction is governed by not only the orbital involved but also the size of anions because the smaller anion, which experiences a lower exchange repulsion is able to approach the π system much closer, which in turn reinforces the orbital overlap and hence leads to the larger induction energy. The inductive type of MO interaction can also be correlated to the extent of charge transfer from the anion to π system. It is important to note that there have been several debates on the role of charge transfer.[35−37] On the basis of some rigorous calculations, Stone and co-workers have conjectured that the charge-transfer interaction cannot be discriminated from the BSSE effect. Indeed, they find that the magnitude of charge tranfer is very small, and in some cases negligible.[38−40]

Nevertheless, in our earlier study on the interaction of cations with π systems,[24] we had indicated that the extent of charge transfer can be correlated to the total induction energy. We have carried out a similar analysis, using the APT charges (Table 4). It can be seen from Figure 4, that in case of the halide anion complexes, the charge transferred from the halide anion to the π system can be correlated to the total induction energies. However, no correlation could be made between the charge-transfer and the total interaction energy.

As mentioned earlier, the magnitude of dispersion energies distinguish these anion$-\pi$ interactions from the corresponding cation$-\pi$ interaction. Though the contribution of dispersion energy to the total interaction energy of the F^- complex with **HFBz** is substantial (36.5%), it increases to about ∼200% for the NO_3^- complex with **TAz**. Apart from the large polarizability of anions, this preeminent contribution of the dispersion interaction could also be attributed to the MO interaction between anions and π systems. In contrast to the case of cation$-\pi$ interaction, it is expected that the anion$-\pi$ interactions would exhibit a different type of molecular orbital (MO) interaction. In the cation$-\pi$ and π-H interactions, we had discussed the role of $\pi-\sigma^*$ interaction (where π is the HOMO of the π system and σ^* is the LUMO of the organic cation or the hydride). This interaction was attributed to the inductive type of interaction. In the case of anion$-\pi$ complexes, this MO interaction is substantially weaker. However, several MO interactions between the occupied orbitals are observed, which are predominantly of the dispersive type (Figure 5). In particular, these interactions are magnified in the complexes involving organic anions with several MO's exhibiting interactions with the HOMOs of the π system.

Despite the large dispersion energies exhibited by these anion$-\pi$ complexes, the total interaction energies of perfluoro$-\pi$ complexes with anions are comparable to those of the corresponding cation$-\pi$ complexes. This implies that the magnitude of the exchange-repulsion energies is substantially

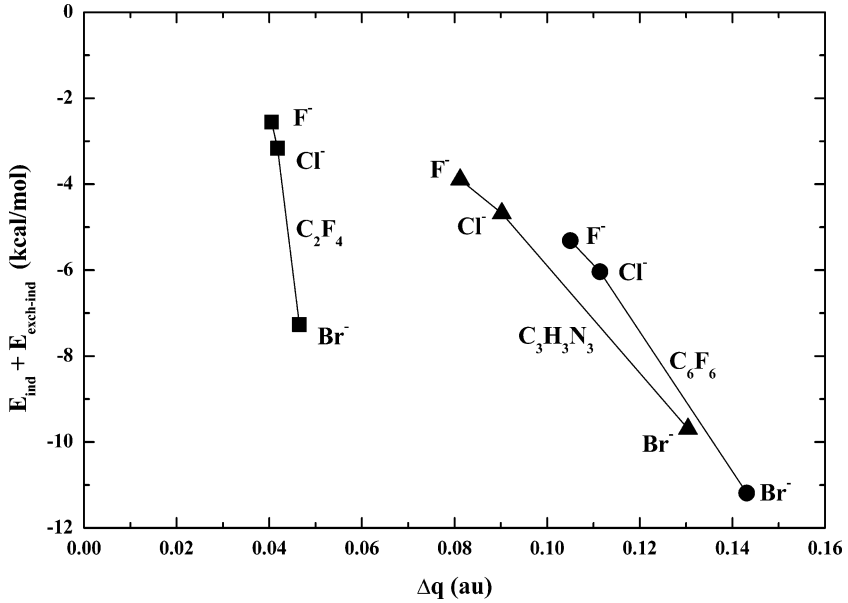

Figure 4. Correlation of the electronic charge transferred from the halide anion to the π system with the total induction energy in the π-halide anion complexes.

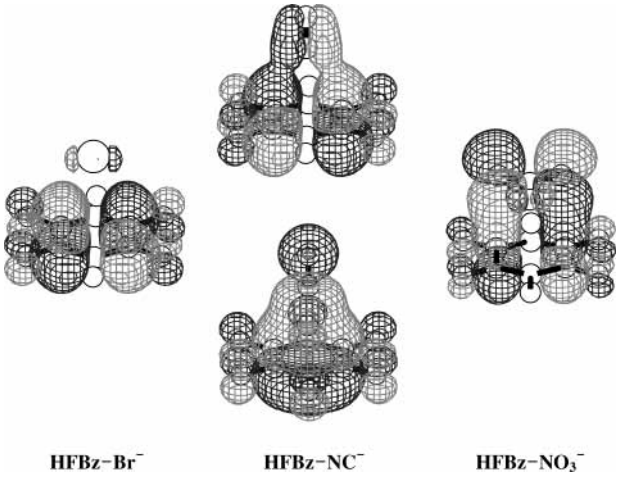

Figure 5. Representative dispersive type of molecular orbital interactions between the highest occupied orbitals of anions and those of C_6F_6. The left one is for the complex of Br^-, the middle ones are for that of NC^-, and the right one is for that of NO_3^-.

higher in case of the anion−π complexes. Compared to the cation, an anion usually possesses an extremely diffuse electron cloud. Though this leads to large increases in the attractive inductive and dispersive energies, the exchange repulsion energy also increases substantially (Figure 3). It is expected that an electron rich anion would be drawn to an electron deficient π system primarily through electrostatic interaction. However, the resulting close orbital overlap apart from enhancing the dispersion energy and reinforcing the induction energy, increases the repulsive exchange interaction.

Because anion−π interactions in real biological systems would exhibit significant deviations from the idealized optimum geometries studied in this report, it would be instructive to examine how the magnitudes of the individual interaction energy components are modulated as the anions approach the π systems from long distances. To this end, we have compared the interaction energy components of the complexes of Cl^- with all three π molecules in this study, and that of CN^- with **FEt** at various intermolecular distances in Figure 6. The three complexes of Cl^- are selected to compare the role of the π systems, and the CN^- complex with **FEt** are chosen because its binding energy is similar to that of the corresponding Cl^- complex (E_{int} of the former is −6.26 kcal/mol and that of the latter −4.99 kcal/mol) so that the examination of their interaction energies would provide a physical picture on the origin of the similar strength of their interactions. At long intermolecular distances, wherein electrostatic interactions dominate the total interaction, the **HFBz** complex shows the strongest interaction, whereas **FEt** complex and **TAz** complex exhibit similar electrostatic interactions. As the distance decreases, induction energies become dominant. The rate of increase of the induction energy is the highest in the **HFBz**−Cl^- complex, and the lowest in the **TAz**−Cl^- complex. This indicates that perfluoro−π systems are more polarizable than **TAz** because the F atoms of the former facilitate the approach of the electron cloud of anion by depleting the electron density in its π cloud. The predomi-

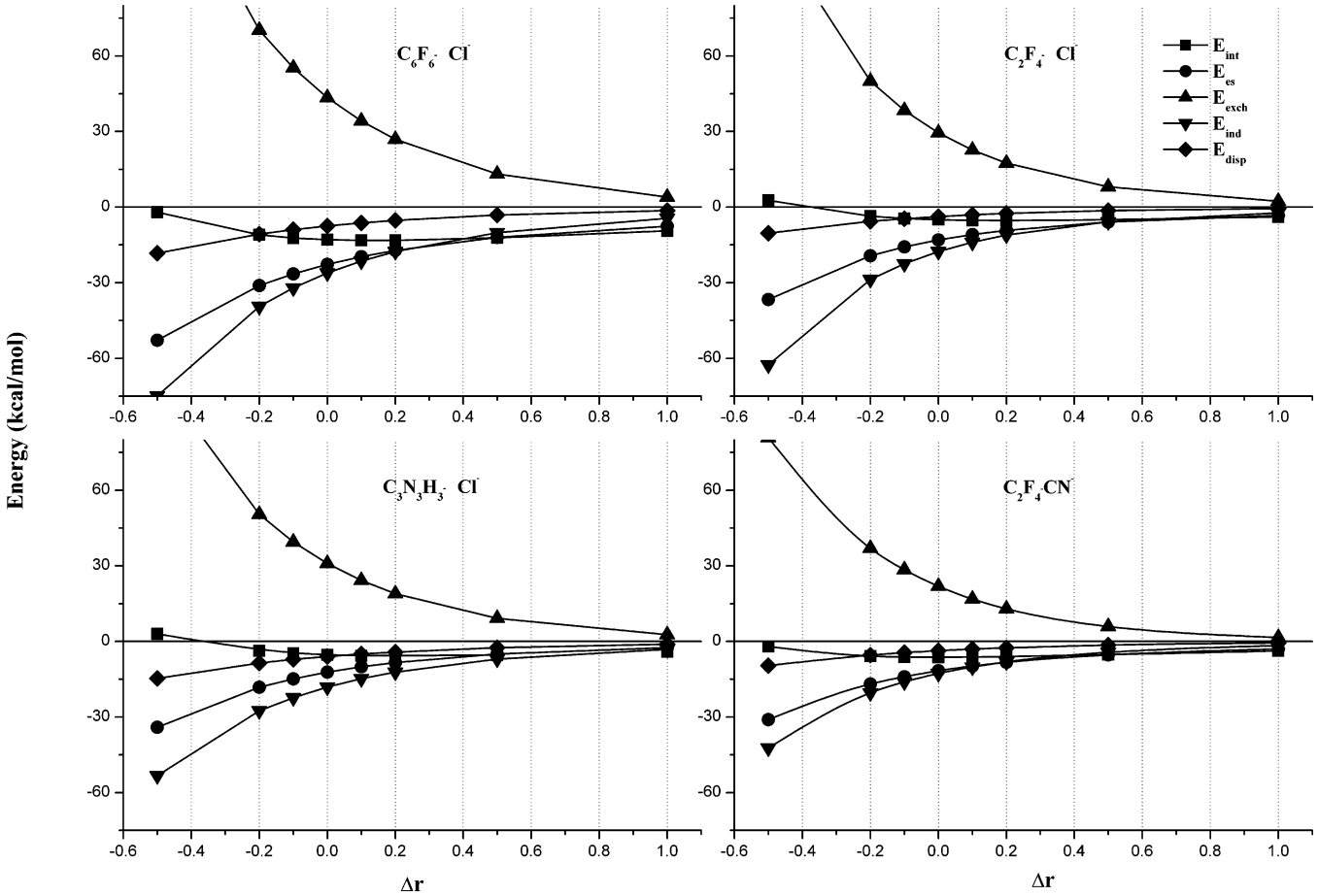

Figure 6. Comparison of the interaction energy components evaluated using the hybrid basis sets for the complexes of Cl^- with C_2F_4, $C_3N_3H_3$, and C_6F_6 and that of CN^- with C_2F_4. See the caption of Figure 2 and the text for the description of various interaction energy terms and the caption of Figure 3 for the description of hybrid basis sets. Δr is the increment in the intermolecular separation, in ångstroms, where $\Delta r = 0.0$ corresponds to that in the equilibrium geometry.

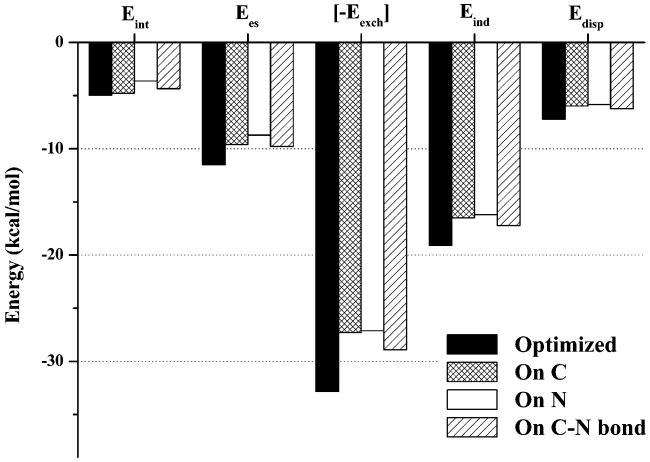

Figure 7. Comparison of the magnitude of the interaction energy components evaluated using 6-31+G* for the $C_3N_3H_3-Br^-$ complex at four different orientations. See the caption of Figure 2 and the text for the description of various interaction energy terms.

nance of the induction energies over the electrostatic energies occur much before the onset of equilibrium geometries in all the Cl^- complexes. The increase in the dispersion energy is larger in the **TAz** complex than in the perfluroethene complex, indicating that the MO interaction of the occupied orbitals are more pronounced in the former. Therefore, the balance of the induction and the dispersion energies is responsible for the similar total interaction energies in the **TAz** and **FEt** complexes because the magnitudes of the electrostatic and the repulsive exchange energies of both are nearly similar and hence cancel out. In comparison of Cl^- and CN^- complexes with **FEt**, several differences can be noted. Except for the dispersion energy, which is similar in magnitude in both complexes, the interaction energy components are larger in the Cl^- complex. The smaller size and the smaller electron density of the C atom of CN^- than of the Cl^- anion are very advantageous for approaching the π system with small exchange repulsion. Because the number of electrons of CN^- is small than that of Cl^- and the most electrons of C atoms reside in the bond region with N atoms, CN^- is expected to have a lower electrostatic interaction with these π systems. On the other hand, because the π orbitals of CN^- facilitate the MO interaction with the HOMOs of the π systems (Figure 5), the magnitude of the dispersion energy is comparable to that of the Cl^- complex.

It is useful to examine the role of the magnitude of various interaction energy components in governing the equilibrium geometry of these complexes, by considering the example of the interaction of Br^- anion with **TAz**. We have evaluated the interaction energy components for four different orientations of the Br^- anion on **TAz**: (i) above the N atom, (ii) above the C atom, (iii) above the CN bond, and (iv) above the center of the **TAz** ring (at the minimal energy conformation). To make an effective comparison, the intermolecular separation observed in the minimal energy conformation was used for all four conformations. The results shown in Figure 7 indicate that the total interaction energy is largest when Br^- is located above the center of **TAz** and smallest when it is located over the N atom. In addition, the dispersion energy (magnitude amounts to around 60% of that of electrostatic energy) is substantial. The difference in the total interaction energies of case (i) and case (ii) mainly results from the difference in the electrostatic interaction energies. This reflects the fact that except for the local charge resulting from the difference of electronegativities of C and N atoms and governing the electrostatic energy, Br^- is rarely able to discriminate the electronic environment at both sites. In the case of CN bond conformation, the magnitude of the electrostatic and the dispersion energies are almost identical to those of the on-C-atom conformation. However, the magnitude of the exchange repulsion energy is much larger than the increase in the inductive energy. This results in the total interaction energy of the CN bond conformation being smaller than that of on-C-atom conformation. Similar observations were made in our earlier study on the interaction in different conformations of K^+-pyrrole complexes.[24] The most interesting thing is, however, the case of optimal conformation. In this case, not only the induction and the repulsive exchange energies but also the electrostatic energy are larger than those of any other conformations.

TABLE 5: Calculated (MP2/631++G) Vibrational Frequency Shifts of the Symmetric Out-of-Plane CF or CH Bending Mode ($\nu^{H\perp}$) of the π System and the Frequencies of the Intermolecular Stretching Mode (S_Z) in All the Anion$-\pi$ Systems[a]**

	C_2F_4		C_6F_6		$C_3N_3H_3$	
	$\nu_4^{H\perp}$	S_Z	$\nu_4^{H\perp}$	S_Z	$\nu_6^{H\perp}$	S_Z
F^-	43_2	150_6	26_4	148_3	-12_0	157_6
Cl^-	30_1	90_2	23_1	106_2	-23_0	104_2
Br^-	27_1	67_1	18_1	76_1	-25_0	77_1
CN^-	39_1	89_3	14_2	109_3	-8_0	100_4
NC^-	39_2	100_4	15_2	118_3	-6_0	117_4
NO_3^-	26_2	99_2	35_2	101_1	2_0	102_2
CO_3^{2-}	-18_{12}	148_{12}	64_6	130_6	-38_2	142_{10}

[a] All the frequencies and frequency shifts are in cm^{-1}. The subscripts beside them are the calculated intensities (10 km/mol). The positive value in $\nu^{H\perp}$ indicates the blue shift, and the negative one does the red shift. The modes are numbered according to Herzberg.[42] The calculated shifts are with respect to the corresponding frequency observed in the uncomplexed monomer {**FEt** = 411_1, **HFBz** = 214_1, and **TAz** = 904_0}.

It would be useful to examine if the binding of anion to the π system exhibits some characteristic spectral signatures. The IR active vibrational frequency shifts of out-of-plane CF or CH bending mode of π systems $\nu^{H\perp}$ and the intermolecular stretching mode S_Z are listed in Table 5. It is of interest to note that **TAz** complexes exhibit red shifts in $\nu^{H\perp}$, whereas perfluoro$-\pi$ complexes exhibit blue shifts. The blue shifts of $\nu^{H\perp}$ were attributed to the exchange repulsion and the consequent steepness of the potential surface, and because the magnitude of exchange repulsion energy is related to the total interaction energy, this type of blue shift was considered an inkling of the strength of interaction.[23,41] In the case of **TAz** complexes, however, even though the exchange repulsion plays a role in determining the amount of the blue shift, the electrostatic interaction between the H atoms of positive partial charge and anions leads to the steepness of potential surface of out-of-plane vibration. Thus, in the case of NO_3^- and CO_3^{2-} complexes, the electrostatic interaction of the latter is stronger than that of the former due to the more concentrated partial charge of the O atoms, even though the O atoms of the latter are close to the H atoms so that the exchange repulsion energy is expected to be higher. The result is that the complex of CO_3^{2-} exhibits the red shift, whereas that of NO_3^- shows a blue shift. Consequently, the red shift of **TAz** complexes is the result of the competition between the attractive electrostatic attraction and the repulsive exchange repulsion. The intermolecular stretching frequency S_Z also yields similar information on the strength of the anion$-\pi$ interaction. For the complexes of the same type of anions, the BSSE and ZPVE binding energies are correlated with the magnitude of the blue shift of S_Z (Figure 8). It would be interesting to experimentally examine the relationship between these spectral features and the interaction energies.

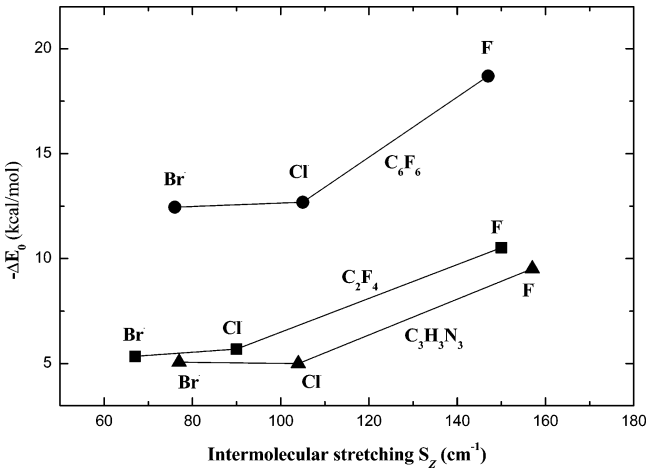

Figure 8. Correlation of the shift of the intermolecular stretching vibrational frequency S_Z with the BSSE and ZPVE corrected interaction energy ΔE_0 in the π−halide complexes.

4. Conclusions

In the present theoretical study, we have investigated the interaction of various anions with several representative π systems. Unlike other complexes containing π systems, computational investigations of anion−π interactions are extremely arduous because of the high levels of theory needed to describe the diffuse nature of both the anion and the π system. A detailed energy decomposition of the anion−π interaction has been carried out to enable a comparison of the magnitude of the individual interaction energy components for different kinds of anion−π interaction and the related cation−π interaction. The salient conclusions, which can be drawn from this study, follow.

1. The total interaction energies of anion−π complexes are comparable to those of the corresponding cation−π complexes.

2. The largest contributions to the total interaction energy in anion−π complexes are the electrostatic and the induction energies.

3. The inductive MO interactions between the highest occupied orbitals of anions and the lowest unoccupied orbital of π systems facilitate the charge transfer from anions to π systems. One can obtain a correlation between the magnitude of the charge transfer and the total induction energy.

4. In contrast to the cation−π interaction, the contribution from the dispersion energies is substantial, and in complexes involving organic anions, their magnitudes are comparable to electrostatic and induction energies. The predominantly large dispersion energy of the organic anion complexes is attributed to the magnified interactions of their occupied orbitals with that of the π systems.

5. Apart from increases in both the induction and dispersion energies, the anion−π interactions are also characterized by a substantial increase in the magnitude of the exchange-repulsion energy.

6. The vibrational frequency shifts of the out-of-plane CF or CH bond bending mode emerge from the competition between the exchange repulsive and the electrostatic interaction of anions and F or H atoms of π systems. The intermolecular stretching vibrations are correlated to the strength of the interaction between anions and π systems.

In the absence of any study on the estimates of the magnitude of the dispersion and repulsion energies, which play a key role in determining the magnitude of interaction energies and the equilibrium geometries of anion−π complexes, the present study would aid understanding of these interactions and also help design novel materials capable of binding anions. We believe that the results presented in this study could be employed to intelligently design and generate crafted molecular systems for size- and molecule-selective processes.

Acknowledgment. This work was supported by the Creative Research Initiative Program of the Korean Ministry of Science and Technology. Partial support was also obtained from the Brain Korea 21 program of the Korean Ministry of Education.

References and Notes

(1) Aviram, A.; Ratner, M. A.; Mujica, V. *Ann. N. Y. Acad. Sci.* **2002**, *960*, 1. Aviram, A.; Ratner, M. A. *Ann. N. Y. Acad. Sci.* **2002**, *852*, 1.
(2) Schon, J. H.; Meng, H.; Bao, Z. *Nature* **2001**, *413*, 713.
(3) Lopinski, G. P.; Wayner, D. D. M.; Wolkow, R. A. *Nature* **2000**, *406*, 48.
(4) Fox, M. A. *Acc. Chem. Res.* **1999**, *32*, 201.
(5) Drain, C. M. *Proc. Natl. Acad. Sci. U.S.A.* **2002**, *99*, 5178.
(6) Kim, H. G.; Lee, C.-W.; Yun, S.; Hong, B. H.; Kim, Y.-O, Kim, D.; Ihm, H.; Lee, J. W.; Lee, E. C.; Tarakeshwar, P.; Park, S.-M.; Kim, K. S. *Org. Lett.* **2002**, *4*, 3971.
(7) Hong, B. H.; Bae, S. C.; Lee, C. W.; Jeong, S. M.; Kim, K. S. *Science* **2001**, *294*, 348. Hong, B. H.; Lee, J. Y.; Lee, C.-W.; Kim, J. C.; Bae, S. C.; Kim, K. S. *J. Am. Chem. Soc.* **2001**, *123*, 10748. Kim, K. S.; Suh, S. B.; Kim, J. C.; Hong, B. H.; Lee, E. C.; Yun, S.; Tarakeshwar, P.; Lee, J. Y.; Kim, Y.; Ihm, H.; Kim, H. G.; Lee, J. W.; Kim, J. K.; Lee, H. M.; Kim, D.; Cui, C.; Youn, S. J.; Chung, H. Y.; Choi, H. S.; Lee, C.-W.; Cho, S. J.; Jeong, S.; Cho, J.-H. *J. Am. Chem. Soc.* **2002**, *124*, 14268.
(8) Choi, H. S.; Suh, S. B.; Cho, S. J.; Kim, K. S. *Proc. Natl. Acad. Sci. U.S.A.* **1998**, *95*, 12094. Choi, H. S.; Kim, D.; Tarakeshwar, P.; Suh, S. B.; Kim, K. S. *J. Org. Chem.* **2002**, *67*, 1848.
(9) Oh, K. S.; Lee, C.-W.; Choi, H. S.; Lee, S. J.; Kim, K. S. *Org. Lett.* **2000**, *2*, 2679.
(10) Suh, S. B.; Cui, C.; Son, H. S.; U, J. S.; Won, Y.; Kim, K. S. *J. Phys. Chem. B* **2002**, *106*, 2061.
(11) Ihm, H.; Yun, S.; Kim, H. G.; Kim, J. K.; Kim, K. S. *Org. Lett.* **2002**, *4*, 2897.
(12) Beer, P. D.; Gale, P. A. *Angew. Chem., Int. Ed.* **2001**, *40*, 486.
(13) Alkorta, I.; Rozas, I.; Elguero, J. *J. Org. Chem.* **1997**, *62*, 4687. Alkorta, I.; Rozas, I.; Elguero, J. *J. Fluorine Chem.* **2000**, *101*, 233.
(14) Danten, Y.; Tassaing, T.; Besnard, M *J. Phys. Chem. A* **1999**, *103*, 3530.
(15) Gallivan, J. P.; Dougherty, D. A. *Org. Lett.* **1999**, *1*, 103.
(16) Kim, K. S. *Proposal of the Creative Research Initiative Program*; Korea Institute of Science and Technology Evaluation, 2000.
(17) Quiñonero, D.; Garau, C.; Rotger, C.; Frontera, A.; Ballester, P.; Costa, A.; Deyá, P. M *Angew. Chem., Int. Ed.* **2002**, *41*, 3389.
(18) Quiñonero, D.; Garau, C.; Frontera, A.; Ballester, P.; Costa, A.; Deyá, P. M *Chem. Phys. Lett.* **2002**, *359*, 486.
(19) Mascal, M.; Armstrong, A.; Bartberger, M. D. *J. Am. Chem. Soc.* **2002**, *124*, 6274.
(20) Alkorta, I.; Rozas, I.; Elguero, J. *J. Am. Chem. Soc.* **2002**, *124*, 8593.
(21) Tarakeshwar, P.; Choi, H. S.; Lee, S. J.; Lee, J. Y.; Kim, K. S.; Ha, T.-K.; Jang, J. H.; Lee, J. G.; Lee, H. *J. Chem. Phys.* **1999**, *111*, 5838. Tarakeshwar, P.; Kim, K. S.; Brutschy, B. *J. Chem. Phys.* **2000**, *112*, 1769. Tarakeshwar, P.; Kim, K. S.; Brutschy, B. *J. Chem. Phys.* **2001**, *114*, 1295.
(22) Tarakeshwar, P.; Kim, K. S.; Kraka, E.; Cremer, D. *J. Chem. Phys.* **2001**, *115*, 6018.
(23) Tarakeshwar, P.; Choi, H. S.; Kim, K. S. *J. Am. Chem. Soc.* **2001**, *123*, 3323.
(24) Kim, D.; Hu, S.; Tarakeshwar, P.; Kim, K. S.; Lisy, J. M. *J. Phys. Chem. A* **2003**, *107*, 1228.
(25) Jeziorski, B.; Szalewicz, K. In *Encyclopedia of Computational Chemistry*; Schleyer, P. v. R., Allinger, N. L., Clark, T., Gasteiger, J., Kollman, P. A., Schaefer, H. F., III, Schreiner, P. R., Eds.; Wiley: Chichester, U.K., 1998. Jeziorski, B.; Moszynski, R.; Szalewicz, K. *Chem. Rev.* **1994**, *94*, 1887. Szalewicz, K.; Jeziorski, B. In *Molecular Interactions − From van der Waals to Strongly Bound Complexes*; Scheiner, S., Ed.; Wiley: New York, 1997; p 3. Jeziorski, B.; Moszyński, R.; Ratkiewicz, A.; Rybak, S.; Szalewicz, K.; Williams, H. L. In *Medium Sized Systems*; Clementi, E., Ed.; Methods and Techniques in Computational Chemistry: METECC-94, Vol. B; STEF: Cagliari, 1993; pp 79−129.
(26) Kim, K. S.; Tarakeshwar, P.; Lee, J. Y. *Chem. Rev.* **2000**, *100*, 4145.
(27) Boys, S. F.; Bernardi, F. *Mol. Phys.* **1970**, *19*, 553.
(28) Cioslowski, J. *J. Am. Chem. Soc.* **1989**, *111*, 8333. Cioslowski, J. *Phys. Rev. Lett.* **1989**, *62*, 1469.
(29) de Oliveira, A. E.; Haiduke, R. L. A.; Burns, R. E. *J. Phys. Chem. A* **2000**, *104*, 5320.

(30) Frisch, M. J.; Trucks, G. W.; Schlegel, H. B.; Scuseria, G. E.; Robb, M. A.; Cheeseman, J. R.; Zakrzewski, V. G.; Montgomery, J. A., Jr.; Stratmann, R. E.; Burant, J. C.; Dapprich, S.; Millam, J. M.; Daniels, A. D.; Kudin, K. N.; Strain, M. C.; Farkas, O.; Tomasi, J.; Barone, V.; Cossi, M.; Cammi, R.; Mennucci, B.; Pomelli, C.; Adamo, C.; Clifford, S.; Ochterski, J.; Petersson, G. A.; Ayala, P. Y.; Cui, Q.; Morokuma, K.; Malick, D. K.; Rabuck, A. D.; Raghavachari, K.; Foresman, J. B.; Cioslowski, J.; Ortiz, J. V.; Stefanov, B. B.; Liu, G.; Liashenko, A.; Piskorz, P.; Komaromi, I.; Gomperts, R.; Martin, R. L.; Fox, D. J.; Keith, T.; Al-Laham, M. A.; Peng, C. Y.; Nanayakkara, A.; Gonzalez, C.; Challacombe, M.; Gill, P. M. W.; Johnson, B. G.; Chen, W.; Wong, M. W.; Andres, J. L.; Head-Gordon, M.; Replogle, E. S.; Pople, J. A. *Gaussian 98*, revision A.1.; Gaussian, Inc.: Pittsburgh, PA, 1998.

(31) Bukowski, R.; Szalewicz, K.; Chabalowski, C. *J. Phys. Chem. A* **1999**, *103*, 7322.

(32) Milet, A.; Moszynski, R.; Wormer, P. E. S.; van der Avoird, A. *J. Phys. Chem. A* **1999**, *103*, 6811.

(33) Visentin, T.; Kochanski, E.; Moszynski, R.; Dedieu, A. *J. Phys. Chem. A* **2001**, *105*, 2023. Visentin, T.; Kochanski, E.; Moszynski, R.; Dedieu, A. *J. Phys. Chem. A* **2001**, *105*, 2031.

(34) Tsuzuki, S.; Honda, K.; Uchimaru, T.; Mikami, M.; Tanabe, K. *J. Am. Chem. Soc.* **2000**, *122*, 3746.

(35) Cubero, E.; Orozco, M.; Luque, F. J. *Proc. Natl. Acad. Sci. U.S.A.* **1998**, *95*, 5976.

(36) Quinn, D. M.; Feaster, S. R.; Nair, H. K.; Baker, N. A.; Radić, Z.; Taylor, P. *J. Am. Chem. Soc.* **2000**, *122*, 2975.

(37) Mo, Y.; Subramanian, G.; Gao, J.; Ferguson, D. M. *J. Am. Chem. Soc.* **2002**, *124*, 4832.

(38) Stone, A. J. *Chem. Phys. Lett.* **1993**, *211*, 101.

(39) Stone, A. J. *The Theory of Intermolecular Forces*; Clarendon Press: Oxford, U.K., 1996.

(40) Kim, K. S.; Lee, J. Y.; Lee, S. J.; Ha, T.-K.; Kim, D. H. *J. Am. Chem. Soc.* **1994**, *116*, 7399. Lee, J. Y.; Lee, S. J.; Choi, H. S.; Cho, S. J.; Kim, K. S.; Ha, T.-K. *Chem. Phys. Lett.* **1995**, *232*, 67.

(41) Engdahl, A.; Nelander, B. *Chem. Phys. Lett.* **1985**, *113*, 49.

(42) Herzberg, G. *Molecular Spectra and Molecular Structure*; van Nostrand Reinhold: New York, 1945; Vol. 2.